Saturation and self-lensing in self-assembled quantum dots with constant-wave driving

A. Tierno and T. Ackemann*
Department of Physics and SUPA, University of Strathclyde, G4 0NG Glasgow, Scotland, United Kingdom

T. Maggipinto and M. Brambilla
Dipartimento Interateneo di Fisica, Universita e Politecnico di Bari, via E. Orabona 4, 70126 Bari, Italy
(Received 30 January 2009; revised manuscript received 9 May 2009; published 22 July 2009)

The nonlinear optical response of self-assembled quantum dots to cw driving is analyzed via numerical simulations of a spatially resolved rate equation model. The saturation is shown to follow a behavior in between the one for a dominantly, homogeneously, and inhomogeneously broadened medium. Self-lensing is suggested to probe the refractive-index nonlinearities and to open a complementary way of characterizing phase-amplitude coupling (α factor) in quantum-dots samples. For conservative assumptions on current samples the minimum focal length is predicted to be ± 1.7 mm for an input beam with 15 μm radius at a detuning of 1.1 inhomogeneous linewidths from gain center.

DOI: 10.1103/PhysRevB.80.035314 PACS number(s): 78.67.Hc, 42.65.Jx

I. INTRODUCTION

Semiconductor quantum dots (QD) are finding considerable interest for laser, amplifier, and quantum information devices (for a recent overview of the field see, e.g., the contributions in the special issues in Refs. 1 and 2). The three-dimensional quantum confinement leads to a "quasiatomic" behavior with a delta-function-like density of states resulting in many realized or anticipated benefits such as low threshold currents, low-temperature sensitivity, and low phase-amplitude coupling. QD size and density can be used in addition to composition to tailor emission wavelengths and other operation characteristics. For example, the 1.3 μm telecommunication band can be reached using the beneficial GaAs material system.

The use of QDs in fast semiconductor saturable absorption mirrors[3] and for ultrafast gain recovery in semiconductor optical amplifiers (SOAs) sparked interest in the transient nonlinear optical properties of QD,[4–6] i.e., under pulsed excitation. As a specific phenomenon in nonlinear beam propagation in two-level systems, self-induced transparency was demonstrated at cryogenic temperatures.[7] Studies on steady-state nonlinear characteristics concentrated on low cryogenic temperatures and single dots due to the relevance for quantum information devices, e.g,[8,9] though some work was done also on QD SOAs at room temperature.[5,10–12]

We are interested in spatial solitons in the regime of diffraction compensation by self-focusing[13] and in particular, in spatial cavity solitons (CS), i.e., self-confined solitary states in cw-driven nonlinear cavities (see Refs. 14–16 for a review). CS are bistable and have "mobility," i.e., are easily being steered around within the device aperture. Hence, they are attractive for all-optical processing applications.[14,17,18] Though CS should exist for self-focusing, absorptive, and even self-defocusing situations, the self-focusing case appears to be the most robust by far.[17,19] Hence the quasiatomic character of the QD susceptibility is beneficial because a self-focusing or self-defocusing situation can be realized by simply changing the detuning whereas a bulk or quantum-well semiconductor is always self-defocusing under absorptive and self-focusing under amplifying conditions. Recent papers address self-organization and cavity solitons in nonlinear resonators based on QD.[20,21] Obviously, this enhanced flexibility of QD might be not only beneficial for solitons but also for nonlinear optics in general.

A convenient way to characterize the nonlinear refractive index is measuring the *lensing* incurred by a spatially varying input beam by the z-scan technique[22] or variants thereof, as done, e.g., for atomic vapors.[23] Measuring the self-lensing provides also an alternative approach to the important problem of characterizing phase-amplitude coupling in QD.[24,25] Due to their symmetric and atomlike gain spectrum, QD should have zero phase-amplitude coupling or linewidth enhancement factor (or α factor[26]) at gain maximum and hence a reduced tendency to instabilities compared to quantum-well and bulk devices. Indeed, a reduced α factor and a reduced tendency to beam filamentation was observed in many QD samples, at least under some operating conditions.[27–30] Characterizing self-lensing will give a direct indication of the tendency of the system to filamentation.

In this paper, we are hence addressing the room temperature, cw nonlinear optics of QDs. Because of the strong coupling of QDs to the semiconductor matrix they are incorporated in, QDs are more complex than "simple" atoms and we are adopting a model including QD and wetting-layer (WL) dynamics with the basic coupling mechanisms using phenomenological rate constants. Another complication comes from the fact that QD spectra correspond to a "Voigt" profile where neither the homogeneous nor the inhomogeneous broadening is strongly dominating. Hence, we will mainly rely on numerical simulations. It turns out that indeed the saturation behavior is in between the expectations for the two limiting cases.

II. THEORETICAL MODEL

Following Refs. 20 and 21 we are modeling the ensemble of QD absorbers as a collection of inhomogeneously broadened two-level systems characterized by a homogeneous linewidth γ_p peaked around a frequency ω_a with coupling to a WL. Carriers in the excited states of the QD (Refs. 11 and

12) are not explicitly taken into account but it is assumed that WL and excited states constitute a common reservoir for the QD ground-state population.[10] Due to the large separation between the lifetimes of the carriers in the QD ground state (100 ps–2 ns) and the fast coupling between the other states to the ground state (100 to some ps)[12,31] the details of this coupling are not very important for the properties of the cw state, if probing and pumping are done at the same frequency. Hence, we will use "QD population" synonymous to "QD ground-state population" and "WL population" synonymous to "WL and excited QD state population" The contribution of each quantum-dot size class is accounted for by a statistical weight

$$G(\Delta_i,\Delta)=\frac{1}{\sqrt{\pi}(\Gamma/\gamma_p)}\exp\left[-\left(\Delta_i-\frac{\gamma_p}{\Gamma}\Delta\right)^2\right], \tag{1}$$

where ω_0 is the frequency of the light field interacting with the QD, $\Delta_i=(\omega_a^c-\omega_0)/\Gamma$ is its normalized detuning from the QD population line center, $\Delta=(\omega_a-\omega_0)/\gamma_p$ is the single dot detuning from resonance and γ_p and Γ are the homogeneous and inhomogeneous broadening parameters.

The equations of motion for the electron and hole population in the QD, n^e, n^h, and in the WL, N^e and N^h, are for driving with linearly polarized light

$$\begin{aligned}\frac{\partial n^{e,h}}{\partial t}=&-\gamma\Bigg[n^{e,h}+\frac{|E|^2}{1+\Delta^2}(n^e+n^h-\Pi)\\&\pm B_{he}N_{\mathrm{WL}}^h n^e(\Pi-n^h)\mp B_{eh}N_{\mathrm{WL}}^e n^h(\Pi-n^e)\\&+\gamma_{\mathrm{esc}}^{e,h}n^{e,h}-\sigma_{\mathrm{cap}}^{e,h}N_{\mathrm{WL}}^{e,h}(\Pi-n^{e,h})\Bigg],\end{aligned} \tag{2}$$

$$\begin{aligned}\frac{\partial N_{\mathrm{WL}}^{e,h}}{\partial t}=&-\gamma^{\mathrm{WL}}\Bigg[-\Lambda+N_{\mathrm{WL}}^{e,h}-\gamma_{\mathrm{esc}}^{e,h}\int n^{e,h}G(\Delta_i,\Delta)d\Delta\\&-\sigma_{\mathrm{cap}}^{e,h}N_{\mathrm{WL}}^{e,h}\int(\Pi-n^{e,h})G(\Delta_i,\Delta)d\Delta\Bigg]\\&\mp B_{he}N_{\mathrm{WL}}^h\int n^e(\Pi-n^h)G(\Delta_i,\Delta)d\Delta\\&\pm B_{eh}N_{\mathrm{WL}}^e\int n^h(\Pi-n^e)G(\Delta_i,\Delta)d\Delta.\end{aligned} \tag{3}$$

Here γ and $\gamma_{nr}^{\mathrm{WL}}$ denote the decay rates of carriers in the QD and the WL, respectively. E represents the optical-field strength, Λ the injection current, $\Pi=2$ the level degeneracy for the two opposite spins. All parameters are suitably scaled.[20,21] The equation for the carrier populations need to be solved for the different size classes, i.e, $n^{e,h}=n^{e,h}(\Delta)$. We use 61 classes in our code. We do not consider coupling between QDs due to diffusion in the WL because the effective diffusion length is not larger than 1 μm (Ref. 32) and we are interested in structures on a larger scale. The terms in the second line of Eq. (2) and the third and last lines of Eq. (3) represent Auger processes coupling the carrier populations in WL and QD. The other coupling processes present in Eqs. (2) and (3) are thermally activated escape from the QD to the WL and the capture of carriers from the WL into the QD. When we account for the energy-level spreading of dots, the capture γ_{esc} and the escape coefficients σ_{esc} can be phrased as[20,21]

$$\gamma_{\mathrm{esc}}=\bar{\gamma}_{\mathrm{esc}}\exp\left(-\frac{\Gamma}{\gamma_p}\beta\Delta_i\right)\exp(\beta\Delta), \tag{4}$$

$$\sigma_{\mathrm{cap}}=\bar{\sigma}_{\mathrm{cap}}\exp\left(\frac{\Gamma}{\gamma_p}\beta\Delta_i\right)\exp(-\beta\Delta), \tag{5}$$

with $\beta=\hbar\gamma_p/k_bT$ (k_bT thermal energy).

The imaginary and real part of the normalized susceptibility describing the strength of light-matter interaction are

$$\mathrm{Im}(\chi_I)=-\int\frac{1}{1+\Delta^2}(n^e+n^h-\Pi)G(\Delta_i,\Delta)d\Delta, \tag{6}$$

$$\mathrm{Re}(\chi_I)=-\int\frac{\Delta}{1+\Delta^2}(n^e+n^h-\Pi)G(\Delta_i,\Delta)d\Delta. \tag{7}$$

Here, for (energetically) deeply buried QDs, we neglected possibly contributions from the WL states and high-level QD states[11,25] in order to elucidate the principles in a first treatment.

Calculations can be performed for the (two-dimensional) case of a surface-emitting geometry or for a (quasi-one-dimensional) edge emitter. We concentrate on the latter because of the smallness of the optical density in a surface emitter. Then, Eqs. (2) and (3) are solved numerically for a cw Gaussian input beam $E(x)=E_0\times\exp(-x^2/w_x^2)$ on a numerical grid with 64 space point and a beam waist w_x of 15 points. Due to the thinness of the active zone in the fast direction (y), $E(x)$ can be taken as the peak value of the field profile of the fundamental mode of the waveguide in the fast direction (with radius w_y) with the form $E(x,y)=E(x)\times\exp(-y^2/w_y^2)$. Note that we do not consider any build-in waveguide in the x direction. The resulting spatial distributions $n^e(x)$ and $n^h(x)$ are then used to calculate the spatial distribution of the susceptibility by Eqs. (6) and (7).

In order to make a connection to experiments, the scaled units need to be related to real ones. The unscaled susceptibility is

$$\chi(\Delta_i,n_e,n_h)=\left(\frac{\mu^2N_{\mathrm{QD}}N_l}{\hbar\epsilon_0\gamma_p d}\right)\chi_I(\Delta_i,n_e,n_h), \tag{8}$$

from which the absorption coefficient for the intensity can be obtained as

$$\alpha_I(\Delta_i,n_e,n_h)=\frac{\omega_0}{n_bc}\mathrm{Im}\ \chi(\Delta_i,n_e,n_h). \tag{9}$$

Here, N_{QD} is the sheet density of QD, N_l is the number of QD layers, d is the total thickness of the active zone, and μ is the dipole-matrix element. In the experiment, one is not measuring the absorption coefficient directly but transmission. Typically, the latter will be integrated over the beam in addition

$$T = \int \exp[-\Gamma_{\text{trans}}\alpha_I(x)L_a]\left(\frac{2}{\pi}\right)^{1/2}\frac{1}{w_x}\exp\left(\frac{-2x^2}{w_x^2}\right)dx, \tag{10}$$

where L_a is the length of the sample and Γ_{trans} is the confinement factor for an edge-emitting structure.

Analogously, the refractive index can be determined from the real part of the scaled susceptibility as

$$n = \langle \Delta n_0 \rangle \text{ Re } \chi_I, \tag{11}$$

where $\langle \Delta n_0 \rangle$ is equal to

$$\langle \Delta n_0 \rangle = \frac{\mu^2}{2n_b\hbar\epsilon_0\gamma_p}\Gamma_{\text{trans}}\frac{N_{\text{QD}}N_l}{d}. \tag{12}$$

Since the input beam is spatially varying, also the refractive index is. Around the beam center, the variation is necessarily parabolic. According to Ref. 33 the radius of curvature acquired by a wave propagating a distance L_a in a medium is given by

$$\frac{1}{R(r)} = \frac{1}{r}\frac{\partial}{\partial r}n(r)L_a. \tag{13}$$

From that we can identify an effective focal power

$$\frac{1}{f}(x) = -\frac{1}{x}\frac{\partial}{\partial x}n(x)L_a, \tag{14}$$

$$= -\langle \Delta n_0 \rangle L_a\left[\frac{1}{x}\frac{\partial}{\partial x}\text{Re } \chi_I(x)\right]. \tag{15}$$

If the refractive-index distribution would be a pure parabola, the focal power would be constant over the whole beam, thus implying an aberration-free equivalent lens. In reality, this is obviously not the case because the pumping Gaussian has an inflection point. Nevertheless the parabola is often a good approximation in beam center where most of the beam energy is. This was studied in detail in atomic vapors[23] and we will discuss it for the QD below. In any case, the curvature will give a quantitative indicator for the strength of beam shaping even if the lens is not perfect. The focusing can be experimentally detected by a change in the beamwidth in far field[34] or at some distance after the medium[23] (similar as in z-scan techniques[22]). In this first treatment, we will confine to a thin lens to demonstrate the principles. For a quantitative description of a real experiment it might be necessary to include absorption and nonlinear beam reshaping during propagation.

We are choosing parameters typical for InGa QD emitting in the 1.3 μm region at room temperature.[5,12,31,35,36] We assume the following set of parameters in normalized units: $B_{eh,he}=200$, $\sigma_{\text{cap}}=500$, $\gamma_{\text{esc}}^{e}=0.01$, $\gamma_{\text{esc}}^{h}=100$, $\gamma_{nr}^{\text{WL}}=0.15$ and a time unit of 11.7 ps. This translates to a rate of (1/160 fs) for the capture and Auger processes coupling the WL to the QD in agreement with measurements for the refilling of the QD ground state from WL and excited states.[12,31]

Other parameters are[5,36,37] $N_{\text{QD}}=5\times10^{10}$ cm^{-2} QD sheet density, $N_l=10$, $d=10\times3.9\times10^{-8}$ m, $\omega_0=1.45\times10^{15}$ s^{-1}, $\lambda=1.3$ μm, $\beta=0.02$, $L_a=1$ mm, $\gamma_p=7.1\times10^{12}$ s^{-1}, and

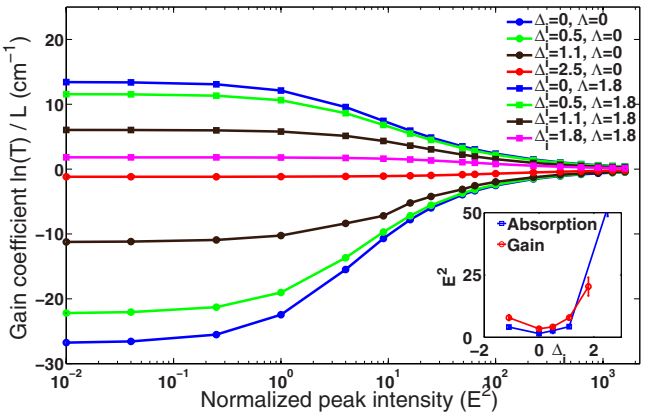

FIG. 1. (Color online) Modal-gain coefficient as a function of the normalized intensity in the center of the Gaussian input beam for different values of the detuning in the absorption (circles) and gain regimes (squares). Detuning increases from bottom to top curve for absorption case (lower part of the figure) and from top to bottom for gain case (upper part of the figure). The inset shows the saturation power as function of the detuning in both cases.

$\Gamma/\gamma_p=4$, corresponding to an inhomogeneous broadening of about 40 nm. A dipole-matrix element of $\mu=1.23\times10^{-28}$ Cm corresponding to a radiative lifetime of $1/\Gamma_1=0.5$ ns results then in a small-signal modal absorption coefficient in line center [Eq. (9) for $n_e=n_h=0$ and $\Gamma_{\text{trans}}=0.094$] of $\langle \alpha_{0,I} \rangle=26$/cm. Since reported small-signal modal-gain values for these structure are between about 19–24/cm in the 1250–1290 nm range[31,36] with small-signal absorption being about 30–100 % larger than the small-signal gain,[31] this is a conservative estimate.

III. RESULTS OF NUMERICAL SIMULATIONS AND DISCUSSION

Figure 1 displays the gain, respectively, absorption coefficient obtained from Eq. (10) in dependence of the input intensity for different detunings. For all curves, it starts at the small-signal value and then drops to the vacuum value of zero due to the generation of carriers and the resulting bleaching. Obviously, the small-signal absorption/gain is highest at $\Delta_i=0$ and decreases for increasing modulus of detuning. The intensity where saturation becomes apparent seems to increase with increasing modulus of detuning.

Since the ratio of $\Gamma/\gamma_p=4$ refers to a Voigt-profile situation where neither homogeneous nor inhomogeneous broadening are clearly dominating, we fit the dependence of the gain coefficient on intensity with different models that describe saturable absorption in the case of two-level systems with inhomogeneous, $\alpha_I=\alpha_{0,I}/\sqrt{(1+E^2/I_{\text{sat}})}$ and homogeneous, $\alpha_I=\alpha_{0,I}/(1+E^2/I_{\text{sat}})$, broadening.[38] The latter proves to fit best the simulation. We show in the inset of Fig. 1, I_{sat} vs Δ_i as extrapolated from the above formula. The saturation intensity is minimal at $\Delta_i=0$ and is slightly different for the gain ($E^2=6.83$) and the absorption case ($E^2=2.99$). It strongly increases in both cases for increasing modulus of the detuning whereas it should be constant in the strongly inhomogeneous limit.[38]

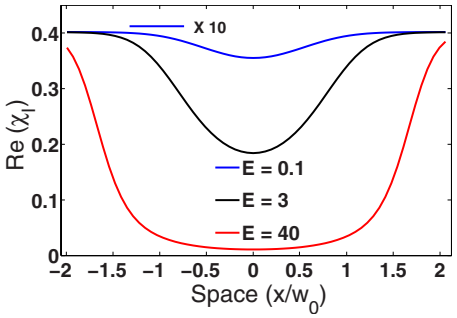

FIG. 2. (Color online) Spatial profile of the real part of the susceptibility for low (upper, blue line, amplitude enhanced by a factor of 10), intermediate (central, black line) and high excitation (lower, red line). $\Lambda=0$, $\Delta_i=1.1$. The total excursion is $\Delta n=1.6\times10^{-4}$.

For an experimental situation with $w_x=15$ μm and $w_y=0.5$ μm, $E^2=1$ corresponds to a power of 2.1 mW. Hence the minimum value of the saturation power is 3 mW in the absorption case and 6.8 mW in the gain case. If instead of $\gamma=0.15$ (or 78 ps lifetime), the purely radiative lifetime is considered, the corresponding values are about a factor of 10 lower and easily accessible experimentally.

Figure 2 shows the spatial profile of the real part of the susceptibility imposed by the Gaussian-pumping profile for low, intermediate, and high peak intensity. For low intensity it follows roughly the Gaussian-intensity distribution of the input beam ("Kerr limit") whereas at high intensities there is a broad plateau in beam center because the beam has sufficient intensity to saturate the sample even in the beam wings. At beam center, the variation is parabolic leading to lensing.

Figure 3 shows how the lens power change as function of input intensity for different detunings in the (a) absorption case as well as in the (b) gain case. Apart from the $\Delta_i\approx0$ case (discussed separately below), the focal power increases from zero with increasing intensity, reaches a peak at an intermediate intensity and decreases again if the intensity is increased further. The sign of the lensing depends on the sign of detuning and whether the sample is absorbing or providing gain, as expected. The maximum lens effect occurs at $\Delta_i=1.1$ and $E^2=9$ ($P=19$ mW). The focal power is maximum at an intermediate input power a few times higher than the saturation power. The intensity needed to obtain maximum lens power increases for increasing modulus of detuning. This is probably due to the fact that the saturation intensity increases with detuning and the maximum effect is found for the same saturation condition.

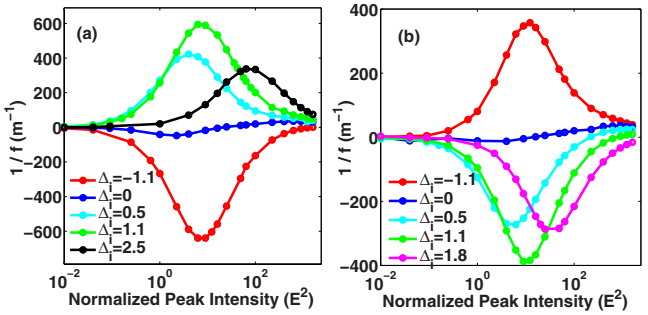

FIG. 3. (Color online) Focal power as function of normalized peak intensity for different detunings in (a) the absorption case and (b) the gain case. ($\Lambda=1.8$ was chosen because it reproduced the experimental finding that maximal gain is about half the absorption coefficient.)

The fact that the maximum focal power is obtained at intermediate input intensity can be explained by looking at Fig. 2. For low intensity the curvature follows the curvature of the input profile ["Kerr limit," $\Delta n(x)\sim|E|^2(x)$] but the total effect is low because the excursion from the background refractive index is small (note that the curve is blown up by a factor of 10). For high intensity, the excursion is large [$\mathrm{Re}(\chi_I)$ becomes nearly zero] but the total focal power is again low because the curvature is strongly reduced. This is due to the fact that saturation is effective over a large area at high intensities. The case of intermediate intensity is in between; on the one hand the excursion is of reasonable size, about half the maximal effect, on the other hand the curvature is still quite close to the one of the input beam. Both is characteristic for intensity levels around the saturation intensity, i.e., for the onset of saturation and hence the total effect is maximal. Similar characteristics were found for atomic vapors.[23] Here, in the homogeneously broadened case, it can be demonstrated analytically that maximum focal power is found at the saturation power.[23]

The lensing effect is minimal at $\Delta_i=0$. Indeed, in a purely two-level system no effect at all is expected for $\Delta_i=0$ because the contributions of blue and red detuned size classes cancel. It is the thermally induced coupling to the WL (described by the parameter β) which breaks that symmetry.

IV. EXPERIMENTAL OBSERVABILITY

In the peak, the predicted lensing effect is actually quite substantial, $|f_{\min}|\approx1.7$ mm, in a sense, because the focal length reaches the length of the medium (assumed to be $L_a=1$ mm), i.e., the point where the approximation by a thin lens becomes questionable. These values were calculated assuming an input-beam radius of $w_x=15$ μm chosen because it would be conveniently to work with experimentally and being somewhat larger than typical fundamental mode sizes in edge-emitting lasers, i.e., in a range where filamentation phenomena might occur. The size of cavity solitons is also in that range [about 10 μm (Refs. 14 and 39)].

Nevertheless, it turns out that an experimental confirmation is not straightforward. The modification of the input beam by the lensing of the sample can be detected by either measuring the on-axis amplitude (being proportional to the square of the new beam waist of the transmitted beam, $w_x'^2$) or the beam width in far field ($\sim1/w_x'^2$) (Ref. 34) or, more sensitively, by measuring the beam size either directly or via the transmission through a pinhole at some suitable chosen distance after the medium as it is done in usual z-scan techniques.[22] Replacing the medium by a thin lens of focal length f, the size of the new beam waist w_x' can be calculated by ABCD-matrix theory as

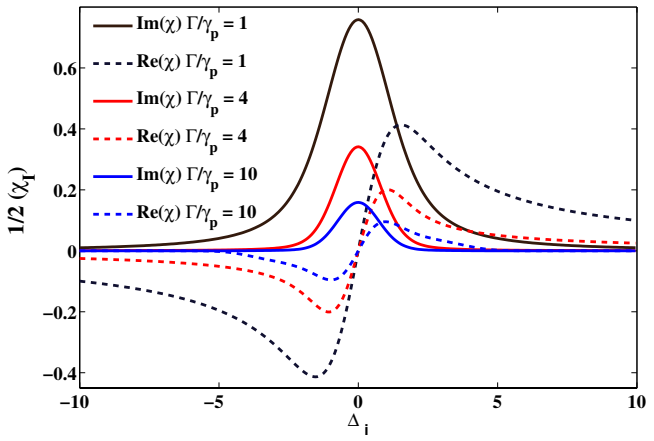

FIG. 4. (Color online) Real and Imaginary part of the linear susceptibility as function of detuning for different ratios between inhomogeneous and homogeneous broadening. The Γ/γ_p ratio decreases from bottom to the top.

$$w_x' = w_x \frac{1}{1 + \frac{\pi w_x^4}{\lambda^2 f^2}}. \tag{16}$$

For an input-beam waist of $w_x = 15$ μm and a thin lens with $f \approx 1.7$ mm, the new beam waist is $w_x = 14.3$ μm at a distance of 0.16 mm. This rather small change in beam is quite difficult to detect. Equation (16) says that the effect becomes more pronounced if the initial beam radius is increased (at constant f), being substantial if the Rayleigh length of the input beam $z_r = \pi w_x^2/\lambda$ is on the order of f. In reality, however, the focal-length scales such as $f \sim w_x^2$, since, as discussed for Fig. 2, the curvature of the susceptibility profile follows the curvature of the input beam in first approximation for not too strong saturation (see Ref. 23 for an analytical treatment). Hence, actually the strength of the detected signal cannot be influenced by choice of the input-beam size.

However, due to the approximately quadratic dependence of the new beam waist on ratio of w_x^2/f, the situation rapidly improves with increasing focal power. For example, a change in size by 20%, which should be experimentally detectable, is reached already for a focal power of about 1000/m, i.e., only about two times the maximum value reported in Fig. 3.

Since it appears that the numbers are somewhat at the edge, it is useful to discuss the influence of other uncertainties, e.g., the exact nature of the relaxation processes between the QD and WL states. First, we changed the ratio between the electron and hole escape from 10^{-4} to 10^{-2} and 1. For detuned excitation ($\Delta_i = 1.1$), the effect on $\mathrm{Re}(\chi_I)$ is negligible and about 22% on $\mathrm{Im}(\chi_I)$. At resonance ($\Delta_i = 0$), the values are 19% on $\mathrm{Re}(\chi_I)$ and 6% on $\mathrm{Im}(\chi_I)$. Switching the Auger processes completely off, on resonance the change in $\mathrm{Im}(\chi_I)$ is 21% and 60% for $\mathrm{Re}(\chi_I)$ (but the total value is very small as discussed above). For $\Delta_i = 1.1$, the change is 64% for $\mathrm{Im}(\chi_I)$ and 7% for $\mathrm{Re}(\chi_I)$.

Figure 4 shows how real and imaginary part of the linear susceptibility change as function of detuning for different ratios between homogeneous and inhomogeneous broadening. Since the linear susceptibility defines the maximum value of the nonlinear index change, this provides a good guidance on the maximum effect to be expected. Choosing a ratio of $\Gamma/\gamma_p = 10$ instead of 4 decreases the maximum of the real part of the susceptibility by a factor of 2.1. For a ratio of $\Gamma/\gamma_p = 1$, it is a factor-of-2 higher. Hence, at constant γ_p, one can expect to benefit from improved growth with a reduced inhomogeneous broadening.[40,41] Note that increasing γ_p at constant Γ is not beneficial because the increase in the scaled susceptibility is sublinear (cf. Fig. 4) and is overcompensated by the dependence of the proportionality factor between scaled and unscaled susceptibility on γ_p, see Eq. (8). We conclude that though uncertainties in the relaxation constants will influence the measurements quantitatively, our overall conclusion that the lensing is at the edge of being detectable is not changed.

Finally, the carrier lifetime in the QD was assumed be 78 ps, much smaller than the radiative lifetime of 500 ps. This was done on the one hand to be on the conservative side with respect to the possible influence of defect-induced recombination and on the other hand to reduce the computational load, which is rather high due to the separation of time scales between scattering processes between WL and QS and carrier lifetime in QD and due to the fact that the carrier density needs to be spectrally and spatially resolved in our case. We did some test runs using a lifetime of 0.5 ns which yield an increase of 10% in saturation and negligible effect in lensing. Note that the influence of the lifetime on the scaling of the saturation power can be treated exactly without additional calculations (as discussed above) due the way the equations are scaled.

V. SUMMARY AND CONCLUSIONS

We calculate the nonlinear optical response of a sample of self-assembled QD to a cw driving field. It is found that a saturation model based on inhomogeneous broadening fits the numerical results but that the saturation power depends on detuning in contrast to a strongly inhomogeneously broadened system. This is interpreted to be due to that fact that QD are in the Voigt-parameter regime between homogeneous and inhomogeneous broadening. From the real part of the susceptibility, the strength of self-lensing is deduced. For conservative assumptions on QD density and carrier lifetimes, the minimum focal length is found to be 1.7 mm for an input beam with a radius of about 15 μm. This effect is probably to small to be experimentally detectable but increasing the focal power by a factor of 2 already changes this conclusions. Due to the uncertainties involved in the parameters, observation seems to be feasible or at least—due to the progress in growth technology[40,41]—promising in the near future. Around the gain peak, lensing is found to be negligible which makes this range promising for the operation of high power lasers with a low tendency to filamentation. Measuring self-lensing might be a convenient way to check out the absolute and relative strength of phase-amplitude coupling (the α factor) for resonant and off-resonant operation.

ACKNOWLEDGMENTS

This work was supported by the EPSRC under Grant No. EP/E025021. We thank Richard Martin for helpful discussions on the numerical simulations. We are grateful to R. Kuszelewicz and S. Barbay for the useful discussions and the earlier collaboration in formulating the model.

*thorsten.ackemann@strath.ac.uk

[1] P. Bhattacharya, D. Bimberg, and Y. Arakawa, Proc. IEEE **95**, 1718 (2007).
[2] M. Sugawara and M. Usami, Nature Photon. **3**, 30 (2009).
[3] D. J. H. C. Maas, A.-R. Bellancourt, M. Hoffmann, B. Rudin, Y. Barbarin, M. Golling, T. Südmeyer, and U. Keller, Opt. Express **16**, 18646 (2008).
[4] T. Akiyama, H. Kuwatsuka, T. Simoyama, Y. Nakata, K. Mukai, M. Sugawara, O. Wada, and H. Ishikawa, Opt. Quantum Electron. **33**, 927 (2001).
[5] A. V. Uskov, E. O'Reilly, M. Laemmlin, N. N. Ledentsov, and D. Bimberg, Opt. Commun. **248**, 211 (2005).
[6] S. Dommers, V. V. Temnov, U. Woggon, J. Gomis, J. Martinez-Pastor, M. Laemmlin, and D. Bimberg, Appl. Phys. Lett. **90**, 033508 (2007).
[7] S. Schneider, P. Borri, W. Langbein, U. Woggon, J. Förstner, A. Knorr, R. L. Sellin, D. Ouyang, and D. Bimberg, Appl. Phys. Lett. **83**, 3668 (2003).
[8] B. Alèn, K. Karrai, R. J. Warburton, F. Bickel, P. M. Petro, and J. Martínez-Pastord, Physica E (Amsterdam) **21**, 395 (2004).
[9] M. H. Baier, E. Pelucchi, E. Kapon, S. Varoutsis, M. Gallart, I. Robert-Philip, and I. Abram, Appl. Phys. Lett. **84**, 648 (2004).
[10] T. W. Berg, J. Mørk, and J. M. Hvam, New J. Phys. **6**, 178 (2004).
[11] M. Sugawara, H. Ebe, N. Hatori, M. Ishida, Y. Arakawa, T. Akiyama, K. Otsubo, and Y. Nakata, Phys. Rev. B **69**, 235332 (2004).
[12] C. Meuer, K. Kim, M. Laemmlin, S. Liebich, A. Capua, G. Eisenstein, A. R. Kovsh, S. S. Mikhrin, I. L. Krestnikov, and D. Bimberg, Opt. Express **16**, 8269 (2008).
[13] G. I. Stegeman and M. Segev, Science **286**, 1518 (1999).
[14] S. Barland *et al.*, Nature (London) **419**, 699 (2002).
[15] W. J. Firth and C. O. Weiss, Opt. Photonics News **13**(2), 54 (2002).
[16] *Dissipative Solitons*, *edited by* N. Akhmediev and A. Ankiewicz, Lecture Notes in Physics Vol. 661 (Springer, Berlin, 2005).
[17] T. Ackemann and W. J. Firth, in *Dissipative Solitons*, edited by N. Akhmediev and A. Ankiewicz, Lecture Notes in Physics Vol. 661 (Springer, Berlin, 2005), pp. 55–100.
[18] F. Pedaci *et al.*, Appl. Phys. Lett. **92**, 011101 (2008).
[19] V. B. Taranenko, G. Slekys, and C. Weiss, in *Dissipative Solitons*, edited by N. Akhmediev and A. Ankiewicz, Lecture Notes in Physics (Springer, New York, 2005), pp. 131–160.
[20] I. M. Perrini, S. Barbay, T. Maggipinto, M. Brambilla, and R. Kuszelewicz, Appl. Phys. B: Lasers Opt. **81**, 905 (2005).
[21] M. Brambilla, T. Maggipinto, I. M. Perrini, S. Barbay, and R. Kuszelewicz, Chaos **17**, 037119 (2007).
[22] M. Sheik-Bahae, A. A. Said, T.-H. Wei, D. J. Hagan, and E. W. V. Stryland, IEEE J. Quantum Electron. **26**, 760 (1990).
[23] T. Ackemann, T. Scholz, C. Vorgerd, J. Nalik, L. M. Hoffer, and G. L. Lippi, Opt. Commun. **147**, 411 (1998).
[24] D. Bimberg and N. N. Ledentsov, J. Phys.: Condens. Matter **15**, R1063 (2003).
[25] S. P. Hegarty, B. Corbett, J. G. McInerney, and G. Huyet, Electron. Lett. **41**, 416 (2005).
[26] C. H. Henry, IEEE J. Quantum Electron. **18**, 259 (1982).
[27] P. M. Smowton, E. J. Pearce, H. C. Schneider, W. W. Chow, and M. Hopkinson, Appl. Phys. Lett. **81**, 3251 (2002).
[28] Z. Xu, D. Birkedal, M. Juhl, and J. M. Hvam, Appl. Phys. Lett. **85**, 3259 (2004).
[29] C. Ribbat, R. L. Selin, I. Kaiander, F. Hopfer, N. N. Ledentsov, D. Bimberg, A. R. Kovsh, V. M. Ustinov, A. E. Zhukov, and M. V. Maximov, Appl. Phys. Lett. **82**, 952 (2003).
[30] S. Schneider, P. Borri, W. Langbein, U. Woggon, R. L. Sellin, D. Ouyang, and D. Bimberg, IEEE J. Quantum Electron. **40**, 1423 (2004).
[31] V. Cesari, W. Langbein, P. Borri, M. Rossetti, A. Fiore, S. Mikhrin, I. Krestnikov, and A. Kovsh, Appl. Phys. Lett. **90**, 201103 (2007).
[32] J. K. Kim, R. L. Naone, and L. A. Coldren, IEEE J. Sel. Top. Quantum Electron. **6**, 504 (2000).
[33] A. E. Siegman, *Lasers* (Science Books, Mill Valley, California, 1986).
[34] G. Labeyrie, T. Ackemann, B. Klappauf, M. Pesch, G. L. Lippi, and R. Kaiser, Eur. Phys. J. D **22**, 473 (2003).
[35] A. Kovsh *et al.*, Electron. Lett. **38**, 1104 (2002).
[36] A. E. Zhukov *et al.*, Physica E (Amsterdam) **17**, 589 (2003).
[37] P. Borri, W. Langbein, J. Mørk, J. M. Hvam, F. Heinrichsdorff, M.-H. Mao, and D. Bimberg, Phys. Rev. B **60**, 7784 (1999).
[38] A. Yariv, *Quantum Electronics*, 3rd ed. (John Wiley & Sons, New York, 1988).
[39] Y. Tanguy, T. Ackemann, W. J. Firth, and R. Jäger, Phys. Rev. Lett. **100**, 013907 (2008).
[40] T. Amano, T. Sugaya, and K. Komori, IEEE Photon. Technol. Lett. **18**, 619 (2006).
[41] C. K. Chia, Y. W. Zhang, S. S. Wong, A. M. Yong, S. Y. Chow, S. J. Chua, and J. Guo, Appl. Phys. Lett. **90**, 161906 (2007).